

Measurements and Performance Factor Comparisons of Magnetic Materials at High Frequency

Alex J. Hanson, Julia A. Belk, Seungbum Lim, David J. Perreault
 Massachusetts Institute of Technology
 77 Massachusetts Avenue, Cambridge, MA 02139, USA
 Email: ajhanson@mit.edu, djperrea@mit.edu

Charles R. Sullivan
 Thayer School of Engineering at Dartmouth
 14 Engineering Drive, Hanover, NH 03755, USA
 Email: charles.r.sullivan@dartmouth.edu

Abstract—The design of power magnetic components for operation at high frequency (HF, 3–30 MHz) has been hindered by a lack of performance data and by the limited design theory in that frequency range. To address these deficiencies, we have measured and present core loss data for a variety of commercially available magnetic materials in the HF range. In addition, we extend the theory of performance factor for appropriate use in HF design. Since magnetic materials suitable for HF applications tend to have low permeability, we also consider the impact of low permeability on design. We conclude that, with appropriate material selection and design, increased frequencies can continue to yield improved power density well into the HF regime.

I. INTRODUCTION

Magnetic components (inductors and transformers) are typically the largest and most lossy components in power converters [1]. While increasing converter switching frequencies can reduce the required size of passive components, size reductions achievable through frequency increases are often limited by core loss (such as in transformers and resonant inductors) [2]; moving beyond operating frequency limits dictated by core loss characteristics can result in unacceptable efficiencies. These concerns have been a significant part of focused research to integrate power supplies “on-chip” (PwrSoC) [3] and “in-package” (PwrSiP) [4] at low power levels, and towards increased miniaturization and integration at higher power levels. In spite of the challenges, recent research has made significant advances in miniaturized power electronics operating in the HF and VHF ranges (3–300 MHz) [5], [6], well above typical modern designs operating from hundreds of kilohertz to a few megahertz.

While such advances have been substantial, the design of power magnetics is still not fully understood or optimized, especially in the high frequency (HF) range (3–30 MHz) where use of low-permeability radio frequency (RF) magnetic materials can play a valuable role. In part, this owes to a lack of data regarding HF magnetic materials. Magnetic materials intended for power conversion are typically characterized for core loss under high flux drive, either by empirically determined graphs relating ac magnetic field amplitude, frequency, and volumetric power loss, or equivalent representations such as Steinmetz parameters. However, large-signal loss data are simply not available for most magnetic materials above a few megahertz, hindering detailed design of power magnetics at these frequencies. Additionally, the modeling and evaluation

methods for magnetic components must be adapted in the HF range. Great efforts have been made to model magnetic core loss and winding loss, but holistic design and evaluation remain incomplete.

In Section II, we discuss the features and limits of the magnetic material *performance factor*, $\mathcal{F} = \hat{B}f$. As traditionally defined, the performance factor assumes that winding loss is independent of frequency, which is often not true in the HF range. We therefore introduce and discuss a *modified performance factor*, $\mathcal{F}_w = \hat{B}f^w$, which is intended to take into account the effects of high-frequency winding loss in the design of magnetic components. The winding parameter w takes on values between $\frac{1}{2}$ and 1 depending on winding design constraints; the choice of $w = 1$ neglects ac effects on winding resistance and returns the traditional performance factor \mathcal{F} .

In Section III, we present core loss data gathered using the method developed in [7] and outlined in the Appendix. These results are meant to fill the aforementioned gap in available loss data and facilitate better magnetics design in the HF range. Results are presented for 14 commercially available materials (mostly NiZn ferrites) for which loss data have not been previously available. The materials span a variety of manufacturers and permeabilities and represent a large proportion of materials available in this space.

In Section IV, the measured data, in conjunction with the limited previous data available from manufacturers and in the literature, are applied to the discussion of performance factor and the modified performance factor presented in Section II, in order to provide some insights into the design of power electronics in the HF range. We further utilize the results from Section III to show the practical impact on the size and quality factor of HF inductors.

In Section V we address the impact of low permeabilities (μ_r from about 4 to 400) on the design of magnetic components, since low permeabilities are common for HF magnetic materials. We introduce the principle of diminishing returns on permeability and conclude that modest permeabilities can be sufficient for effective magnetic component design at HF frequencies.

Section VI presents our general conclusions. In particular, we foresee significant power density improvements for power magnetics operating well into the HF range.

II. PERFORMANCE FACTORS

A popular way to evaluate the capability of power magnetic materials across a range of frequencies is the “performance factor” [8]–[17]

$$\mathcal{F} = \hat{B} \cdot f \quad (1)$$

where f is the frequency of operation under consideration and \hat{B} is the peak amplitude of ac flux density that results in a specified power loss per unit volume P_v , taken to be the maximum practical allowable power dissipation per unit volume. Typical values of P_v are 200 mW/cm³ (a conservative value), 300 mW/cm³ (a moderate value), or 500 mW/cm³ (for small volumes, planar geometries, and/or active cooling). Performance factor is designed to be proportional to the power or VA handling possible with a given core, and is relevant as a design metric for applications such as transformers and resonant inductors where core loss is a major design constraint.

Performance factor is developed considering limitations on power loss for a given core size, under several assumptions. The first assumption is to neglect variations in ac winding resistance (and hence winding loss) with frequency such that, for a given winding, the achievable ampere-turns (NI_{max}) is independent of the frequency. The second assumption is that the waveform shapes are sinusoidal, and the third assumption is that the flux density is limited by power loss in the core, not by saturation. Because the instantaneous voltage across a winding is proportional to dB/dt , the maximum rms value of the voltage at a given power loss per volume P_v is proportional to magnetic flux density and frequency, $V_{max} \propto \hat{B} \cdot f$. Given fixed waveform shapes, the power or VA is proportional to the product of rms current and voltage, and thus to the performance factor.

$$VA = V_{max} I_{max} \propto (\hat{B}f) \times (I_{max} = \text{constant}) \propto \mathcal{F} \quad (2)$$

A plot of performance factor as a function of frequency for a collection of materials provides a quick way to compare materials and identify the highest performance materials at a given frequency, or to identify the frequency range where a particular material is most useful. However, the assumptions underlying the traditional performance factor impose some limits on its usefulness, and some modified performance factors have been proposed to overcome these limits. In [18], a modified performance factor is proposed to consider saturation flux density also. The proposal is to simply take the geometric mean of saturation flux density (a consideration for dc current) and conventional performance factor (a consideration for ac current) to obtain $\mathcal{F}_{dc+ac} = \sqrt{B_s \cdot \mathcal{F}}$. Although no rigorous justification is given for this formulation, it appears to be useful in design examples provided in [18]. In [19], another modified performance factor is proposed, $\mathcal{F}_{\frac{3}{4}} = \hat{B}f^{\frac{3}{4}}$. The $\frac{3}{4}$ exponent is said to account for high-frequency winding effects.

At MHz frequencies, high-frequency winding effects are consistently important, and magnetics design is often dominated by core loss rather than saturation considerations. Thus, we choose to examine $\mathcal{F}_{\frac{3}{4}}$ in more detail. First we note that for comparing different materials at a fixed frequency, the choice

between conventional (\mathcal{F}) and modified ($\mathcal{F}_{\frac{3}{4}}$) performance factors does not matter – either will lead to the same conclusions as they differ by only a fixed factor of $f^{\frac{1}{4}}$. However, if the goal is to select an operating frequency, they may lead to different conclusions, with \mathcal{F} indicating a larger benefit to increasing frequency, but with that advantage discounted based on high-frequency winding loss when $\mathcal{F}_{\frac{3}{4}}$ is used.

We extend the theory in [19] and designate $\mathcal{F}_w = \hat{B}f^w$ as the modified performance factor, where w is a parameter selected based on the analysis of winding loss in each case. The choice of $f^{\frac{3}{4}}$ in [19] is based on the assumption that $R_{ac} \propto f^{\frac{1}{2}}$, as is the case with simple skin effect. To maintain a constant power loss in a given winding, the maximum current handling is proportional to $\sqrt{R_{ac}}$, which is proportional to $f^{-\frac{1}{4}}$. More generally, for fixed loss with varying numbers of turns, $I \propto f^{-\frac{1}{4}}/N$. The voltage is proportional to $N\hat{B}f$, so the product of voltage and current is proportional to $\hat{B}f^{\frac{3}{4}}$. Hence $\mathcal{F}_{\frac{3}{4}}$ is appropriate for components with windings whose ac resistance is determined by simple skin effect, and thus is a good choice for use in the HF range.

However, in many practical situations the assumption that winding resistance is dominated by skin effect is not valid. In particular, for multi-layer windings including litz wire windings, proximity effect is also important. To determine the appropriate type of modified performance factor to use for these cases, we assume that the winding is optimized for the particular frequency to be used. As discussed in [20], there are several possible constraints one might adopt for optimizing a multi-layer winding, so we consider each in turn to find the corresponding modified performance factor, $\mathcal{F}_w = \hat{B}f^w$. The results, derived below, are listed in Table I.

One scenario is a multi-layer winding with a fixed number of layers, and with the conductor thickness in each layer optimized to minimize ac resistance at the operating frequency. This is Case 2 in [20] and is also the case considered in the winding optimization analysis in [21]. The result, for p layers, is an optimized winding resistance that is a factor of $1/\sqrt{p}$ lower than the resistance of a single-layer winding, using a layer thickness of approximately $1.3\delta/\sqrt{p}$. Thus, the frequency dependence is the same as for a single-layer winding, which is simply the case in which the fixed value of p is equal to 1, and for any fixed value of p , the appropriate modified performance factor is $\mathcal{F}_{\frac{3}{4}} = \hat{B}f^{\frac{3}{4}}$.

Unfortunately, for frequencies in the HF range, the optimum thickness for a many-layered winding can be thinner than is easily practical. Litz wire becomes very expensive with strands smaller than 50 μm in diameter and is not commercially available with strands smaller than about 30 μm . Although foil is available at low cost down to single-digit micrometer thicknesses, applying it effectively in multiple parallel layers can be difficult [22]. Thus, another situation of interest is a minimum thickness constraint on the layers of a multi-layer winding. In this case, as reviewed in [20], the resistance is reduced relative to the resistance of a single-layer winding by a factor of about $\frac{2}{3} \frac{t_{min}}{\delta}$, where t_{min} is the minimum thickness

constraint and δ is the skin depth, for thicknesses below about 1.5 skin depths. Given that the resistance of a single-layer winding is proportional to $1/\delta$, we see the the optimized multi-layer design under this constraint has resistance proportional to $1/\delta^2$, and thus proportional to frequency. As shown in Table I, this results in a modified performance factor $\mathcal{F}_{\frac{1}{2}} = \hat{B}f^{\frac{1}{2}}$. It is important to note this this is only valid for combinations of frequency and minimum thickness such that $t_{min} < 1.5\delta$; beyond that point, a single layer would be preferable, and $\mathcal{F}_{\frac{3}{4}}$ should be used instead.

A particular example of this is litz wire for which we take AWG 48 or $32\mu\text{m}$ as the smallest practical strand diameter. The corresponding effective layer thickness is $0.584d_{min}$ [20], or $18.7\mu\text{m}$. This is equal to 1.5δ at 28 MHz at room temperature in copper, indicating in this case that magnetic materials could be evaluated using $\mathcal{F}_{\frac{1}{2}}$ for frequencies up to 28 MHz. The lower power of f ($\frac{1}{2}$ instead of $\frac{3}{4}$) in the performance factor for this case indicates the diminishing value of litz wire over the HF frequency range, and in practice, litz wire is not usually worthwhile above the low end of the HF range (though it has been used effectively in the 5–10 MHz range, e.g., [23], [24]).

A third case is a multi-layer winding with a fixed number of wire strands, and with the strand diameter optimized. With the number of strands n fixed at one, this corresponds to a simple solid-wire winding. Larger values of n correspond to litz wire with a fixed number of strands. As the diameter of the strands is varied, the number of turns that fit in one layer of the winding varies, and so the number of layers varies. Thus, this case is different from the case of a fixed number of layers. Designs optimized under this constraint have a ratio of ac resistance to dc resistance $F_r = 1.5$, and wire diameter proportional to $1/f^{\frac{1}{3}}$ [25], [26]. This results in ac resistance proportional to $f^{\frac{2}{3}}$, and $\mathcal{F}_{\frac{2}{3}} = \hat{B}f^{\frac{2}{3}}$. In the HF range, multi-layer solid-wire windings are a poor choice and litz wire is limited by strand diameter rather than by the feasible or economical number of strands. Thus, this version of modified performance factor is more relevant to the low frequency (LF) range (30–300 kHz) than to the HF range, but it is included in Table I for completeness.

A final case to consider is one in which an advanced winding technology eliminates skin- and proximity-effect losses and makes the ac resistance equal to the dc resistance, and the achievable winding resistances is not limited by number of strands, number of layers, or a minimum thickness constraint, but instead by the available space in the winding window. In this case, the ordinary performance factor \mathcal{F} is the appropriate measure, just as it is for lower frequency designs where skin and proximity effects are not significant. For example, at tens of kilohertz, litz wire can perform well enough in many cases that an initial design can be based on the assumption that skin and proximity effect are eliminated, although care is needed in the litz wire design to ensure that this goal is achieved [27]. For HF windings, skin and proximity effect are still serious issues even with the best available litz wire. Possible methods to make HF windings that approach the performance of litz

TABLE I: Optimized ac resistance as a function of frequency for different assumptions and resulting performance factor formulation

Case	R_{ac} vs. f	NI vs. f	Corresponding performance factor
No significant ac resistance effects	$R_{ac} \propto f^0$	$NI \propto f^0$	$\mathcal{F}_1 = \hat{B}f$
Single-layer winding or other fixed number of foil layers or effective wire layers	$R_{ac} \propto f^{\frac{1}{2}}$	$NI \propto f^{-\frac{1}{4}}$	$\mathcal{F}_{\frac{3}{4}} = \hat{B}f^{\frac{3}{4}}$
Fixed layer or strand thickness	$R_{ac} \propto f$	$NI \propto f^{-\frac{1}{2}}$	$\mathcal{F}_{\frac{1}{2}} = \hat{B}f^{\frac{1}{2}}$
Fixed number of wire strands with many layers	$R_{ac} \propto f^{\frac{2}{3}}$	$NI \propto f^{-\frac{1}{3}}$	$\mathcal{F}_{\frac{2}{3}} = \hat{B}f^{\frac{2}{3}}$

wire at lower frequencies are discussed in [22].

The different performance factors in Table I can be summarized as follows:

- Without significant ac resistance effects, conventional performance factor is appropriate.
- With ac resistance effects, and with a single-layer winding, as is often the most practical solution for frequencies in the HF range, the appropriate modified performance factor is $\mathcal{F}_{\frac{3}{4}}$. This result also applies to any fixed number of layers, if the thickness of the layers is optimized for the frequency of operation.
- If the fixed constraint is instead the minimum layer thickness or wire diameter, and the number of layers or strands is optimized for the frequency of operation, the appropriate performance factor is $\mathcal{F}_{\frac{1}{2}}$.
- The intermediate case of a multilayer wire winding with a fixed number of strands results in $\mathcal{F}_{\frac{2}{3}}$, but is rarely relevant to the HF range.

Thus, in our generalized definition of high-frequency performance factor $\mathcal{F}_w = \hat{B}f^w$, we choose values of w between $\frac{1}{2}$ and 1 based on the winding design constraints anticipated in the application of interest. Because a single-layer winding is the most common choice for frequencies in the HF range, we choose to use $w = \frac{3}{4}$, and thus $\mathcal{F}_{\frac{3}{4}} = \hat{B}f^{\frac{3}{4}}$ for comparing core materials in Section IV (in addition to traditional performance factor $\mathcal{F} = \hat{B}f$). Nevertheless, for specific types of winding designs and different frequency ranges, the different modified performance factors listed in Table I can be chosen accordingly.

III. MEASURED CORE LOSS DATA

In order to use the performance factor in its original or modified form it is necessary to have core loss data for a variety of materials across the frequency range of interest. As discussed in the introduction, there is a significant lack of core loss data available in the HF range. Datasheets include core loss data for materials up to a few megahertz [28], and the literature contains some sparse data in the VHF (30–300 MHz) range [7]. Core loss data in the HF range are necessary for

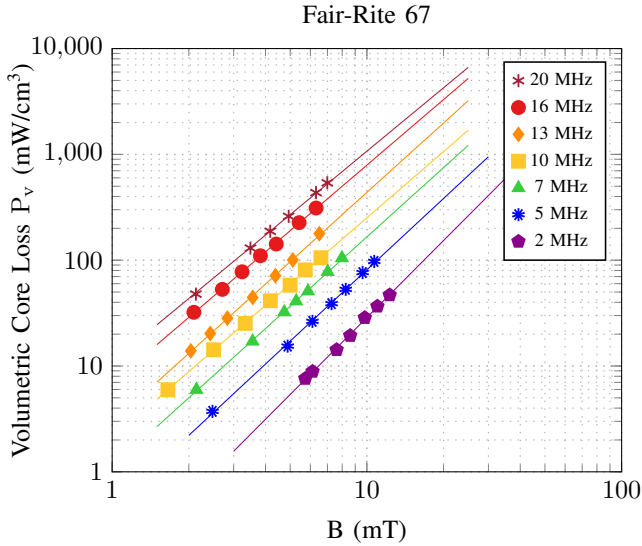


Fig. 1: Core loss data from Fair-Rite 67 as a sample material suitable for HF operation. Fair-Rite 67 has a nominal relative permeability $\mu_r = 40$.

design in general and to apply theoretical extensions like those in Section II.

Using the method described in the Appendix, we have measured core loss characteristics for materials of various types and permeabilities from a variety of manufacturers. Data were primarily gathered in the range of 2–30 MHz, as this represents the greatest dearth in available data. Core loss data with fitted curves can be shown graphically as in Fig. 1.

Core loss data can also be represented algebraically by the Steinmetz equation, $P_v = k\hat{B}^\beta$, where k and β are known as the Steinmetz parameters [29]. Parameters for materials are empirically determined by curve fitting from the same experimental data used to create loss charts like those in Fig. 1. In this formulation of the Steinmetz equation, independent values of k and β are required for each frequency. Values of k and β for all measured materials at all measured frequencies are listed in Table II.

IV. EXPERIMENTAL PERFORMANCE FACTOR ANALYSIS AND COMPARISON

Performance factor \mathcal{F} and modified performance factor $\mathcal{F}_{\frac{3}{4}}$ were calculated from the measured core loss data in Table II. The magnetic flux densities corresponding to a loss density of $P_v = 500 \text{ mW/cm}^3$ were found and used to compute the performance factor $\mathcal{F} = \hat{B}f$ and modified performance factor $\mathcal{F}_{\frac{3}{4}} = \hat{B}f^{\frac{3}{4}}$. The standard and modified performance factors are plotted in Figures 3 and 4 respectively.

Performance factor data are also included from Ferroxcube [28], with modified performance factor calculated from the listed data as $\mathcal{F}_{\frac{3}{4}} = \mathcal{F}/f^{\frac{1}{4}}$. These data come from MnZn ferrites optimized for different frequency ranges, and one NiZn ferrite material (4F1), and are representative of available materials at low frequency. Each point on the Ferroxcube curve

represents the highest performance factor among Ferroxcube materials at a particular frequency. Both standard and modified performance factors are also calculated for the VHF data presented in [7].

Fig. 3 shows that the maximum performance factor of available materials increases roughly as the square root of frequency between 20 kHz and 100 kHz, providing a good opportunity for improved power density through increasing frequency in that range. Between 100 kHz and 2 MHz, the improvement rate is slower, and is on average approximately proportional to frequency to the 0.25 power. This indicates that, although increasing frequency can be advantageous for reducing magnetics size, the benefits are not as large in this range. This is particularly true when winding loss is also considered, as reflected in the modified performance factor plotted in Fig. 4, where little if any benefit is seen in the 100 kHz to 2 MHz range. However, both plots show substantial improvements above 2 MHz using some materials that have not been previously widely used in power conversion applications.

Moving from 2 MHz to 10 MHz, the best standard performance factor increases by a factor of approximately two, and the best modified performance factor increases by a factor of 1.45. Thus, for typical HF inductors or transformers with single-layer windings, we can expect a 45% increase in power density (in a power-loss-density limited design) to result from an increase in frequency from 2 MHz to 10 MHz. This same increase would also apply with an advanced winding technology limited by the number of winding layers. With a hypothetical winding technology that made skin and proximity effects negligible, without being constrained in the number of layers used or their thickness, the full factor-of-two improvement would be available.

In order to illustrate the effect of operating frequency on magnetics size using a given core material, inductors were designed for constant impedance at various frequencies, allowing volume to scale to maintain Q constant. The inductors were designed with single-layer foil windings on ungapped cores in a low-permeability RF magnetic material (Fair-Rite 67, $\mu_r = 40$), targeting an impedance of approximately 35Ω at a quality factor of approximately 200, at a current handling of 1.6 A (ac peak). The results are demonstrated in Fig. 2. Ungapped inductors lack the degree of design freedom from the gap length and toroids are only available in certain fixed sizes, and therefore the illustrated designs are not fully optimized. However, the fact that the inductor loss is dominated by the core rather than the windings serves to highlight the *material* properties, and illustrates the general core selection tradeoffs. As can be seen in Fig. 2, the power density vs. frequency at constant impedance and loss improves significantly (by a factor of 3) from the 3.5 MHz design to the 9 MHz design, but then quickly declines. Minimum inductor volume (highest power density) is achieved in the frequency range where material performance factor peaks.

From this example we see that operating at frequencies best suited to a given magnetic material can offer significant

TABLE II: Steinmetz parameters for commercially available HF materials, valid for $P_v(\text{mW}/\text{cm}^3) = k \times B(\text{mT})^\beta < 1000$

Material	Frequency→	2 MHz		5 MHz		7 MHz		10 MHz		13 MHz		16 MHz		20 MHz	
	μ_r	k	β	k	β	k	β	k	β	k	β	k	β	k	β
Ceramic Magn. C2025	175	0.49	2.67	3.14	2.58	11.33	2.27	30.15	2.20	-	-	-	-	-	-
Ceramic Magn. C2050	100	0.52	2.9	2.47	2.75	5.25	2.76	12.44	2.50	-	-	-	-	-	-
Ceramic Magn. CM5	290	0.61	2.66	9.42	2.29	22.55	2.19	42.04	2.08	-	-	-	-	-	-
Ceramic Magn. N40	15	-	-	1.52	2.09	3.04	2.00	6.61	2.01	11.09	2.02	12.47	2.06	21.20	2.04
Ceramic Magn. XTH2	80	-	-	0.83	2.82	1.72	2.72	3.86	2.68	7.07	2.57	15.20	2.57	42.00	2.38
Fair-Rite 52	250	0.46	2.97	5.44	2.53	14.44	2.32	-	-	-	-	-	-	-	-
Fair-Rite 61	125	0.08	2.79	0.42	2.67	0.83	2.62	1.80	2.56	4.31	2.47	6.66	2.53	-	-
Fair-Rite 67	40	0.10	2.44	0.69	2.20	1.11	2.18	2.09	2.08	2.91	2.18	6.06	2.04	10.95	1.99
Ferroxcube 4F1	80	0.15	2.57	1.11	2.27	-	-	2.86	2.28	6.53	2.09	10.89	2.05	23.20	2.14
Metamagnetics HiEff 13	425	0.11	3.06	10.44	2.10	12.69	2.32	-	-	-	-	-	-	-	-
Micrometals 2	10	-	-	-	-	-	-	10.97	2.09	19.32	2.07	28.79	2.04	57.09	2.00
National Magn. M	125	0.03	3.36	0.45	2.83	1.35	2.69	2.52	2.57	5.23	2.56	-	-	-	-
National Magn. M3	20	-	-	0.85	2.10	1.66	2.03	2.55	2.05	4.87	1.95	7.54	2.01	14.44	1.98
National Magn. M5	7.5	-	-	-	-	90.34	2.14	147.6	2.17	198.3	2.21	225.1	2.12	335.1	2.15

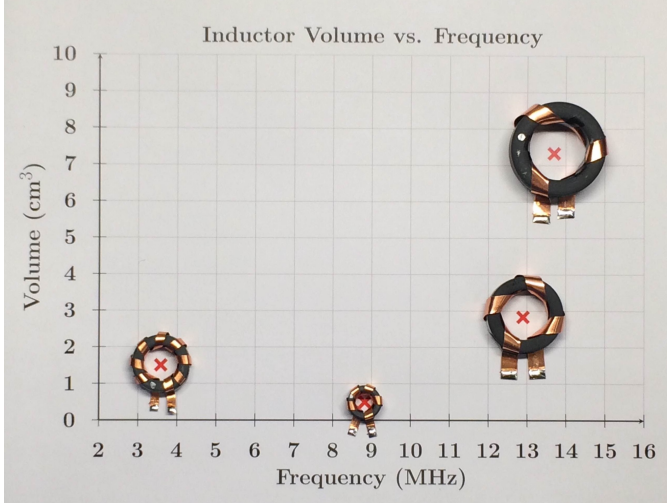


Fig. 2: Inductors using ungapped toroidal cores in Fair-Rite 67 material ($\mu_r = 40$) designed for sinusoidal current at an impedance level of approximately 35Ω and a quality factor of approximately 200 (see Table III). The figure illustrates the inductor volume vs frequency at a given quality factor. Minimum inductor volume (highest power density) is achieved in the frequency range where material performance factor peaks.

TABLE III: Power inductors designed for identical impedance and large-signal quality factor at an ac current of 1.6 A, corresponding to those in Fig. 2.

Frequency MHz	Impedance Ω	Large-Signal Q	Volume cm^3	P/N
3.58	36.5	212	1.50	5967001801
8.83	33.7	193	0.49	5967001101
12.90	33.4	220	2.83	5967001001
13.70	39.9	202	7.33	5967002701

benefit in power magnetic component design. Moreover, taken together with the data in Figs. 2 and 3, we can conclude that significant improvements in the power density of cored power magnetic components (those that are limited in performance by core loss) can be achieved by moving into the HF regime (e.g., at least up to 10 MHz with available magnetic materials).

Improvements in main power stage magnetics are not the only advantages of higher-frequency operation for magnetic components and circuit design. For example, the size of magnetic components associated with filters (e.g., for EMI) are often not determined by core loss considerations, but rather by required filter cutoff frequency, such that increased operating frequency can yield very rapid reductions in component size. Since the EMI filter for a grid-interface converter can often consume 20% or more of system volume, frequency increases into the HF regime can help substantially reduce filter size and overall converter size. (This effect is illustrated in the design in [24], where EMI filter size is extremely small owing to operation in the 5–10 MHz range; indeed the volume of the entire converter is smaller than the EMI filter alone required for a typical 100 kHz-range design). Likewise, as illustrated in [2], switching frequency increases (and the smaller associated inductance and capacitance values) can aid in substantially improving transient response speed of power converters.

V. PERMEABILITY

Most magnetic materials suitable for HF operation have relatively low permeabilities ($\mu_r < 250$), with some of the highest performance factors achieved with $\mu_r \approx 40$ (Fig. 5). High relative permeability μ_r is sometimes thought of as being important for the design of magnetic components; however, neither the traditional performance factor \mathcal{F} nor the modified performance factor $\mathcal{F}_{\frac{3}{4}}$ directly depend on the material permeability. It is natural to inquire whether the low-permeability materials available are effective in practice for power magnetic

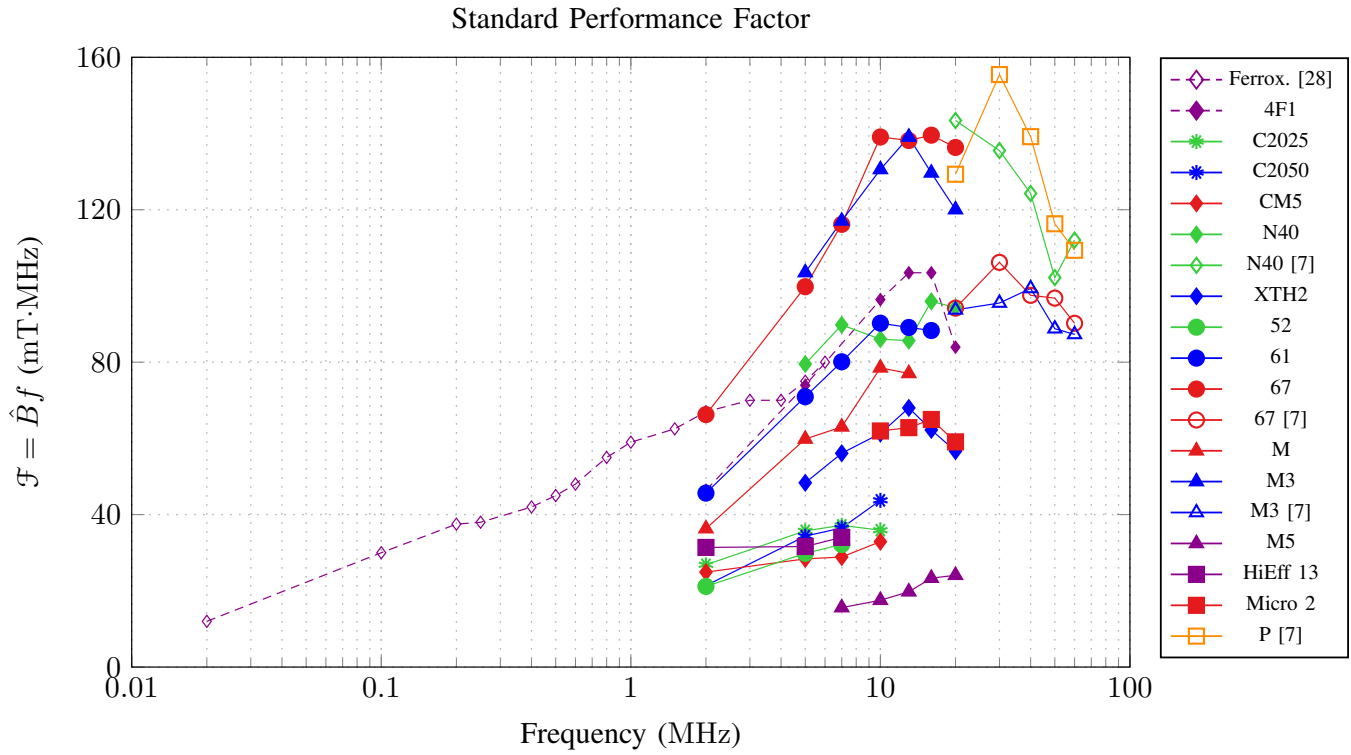


Fig. 3: Survey of standard performance factor, incorporating data from industry, the literature, and this work.

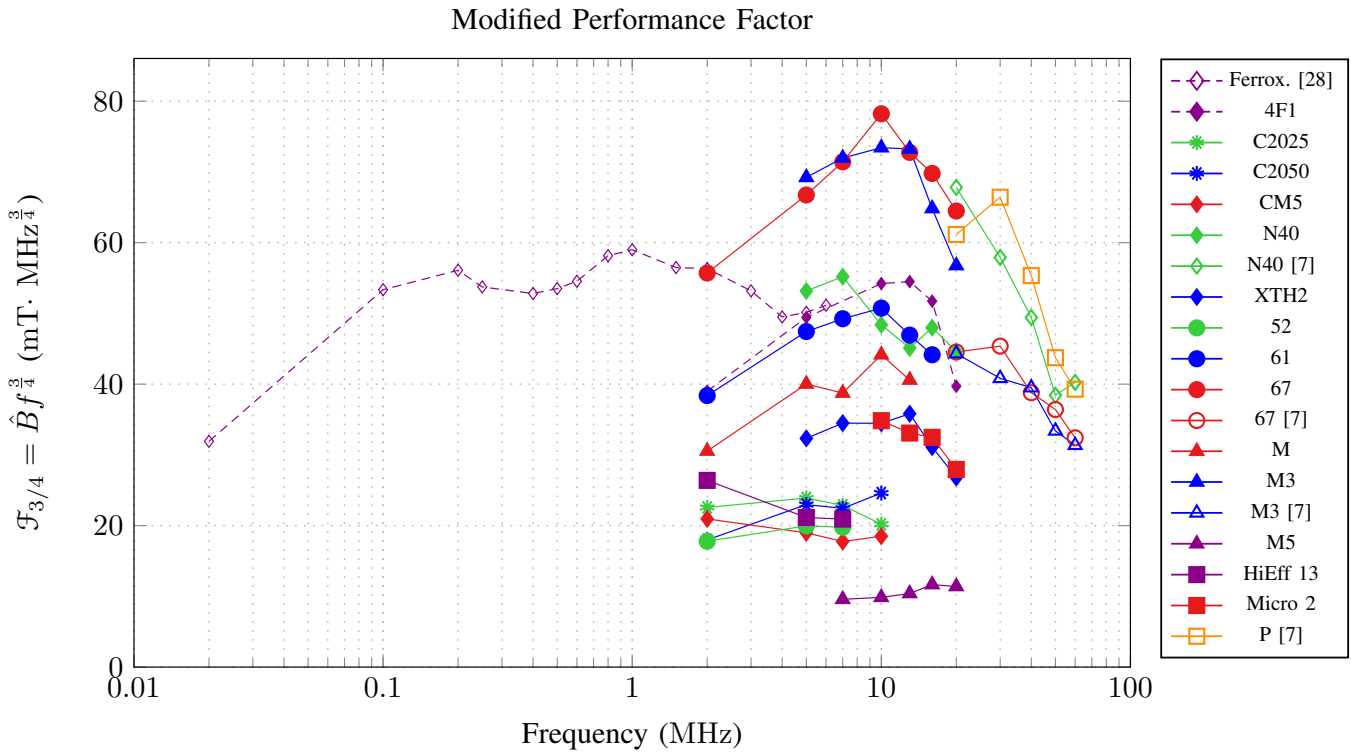


Fig. 4: Survey of modified performance factor, incorporating data from industry, the literature, and this work.

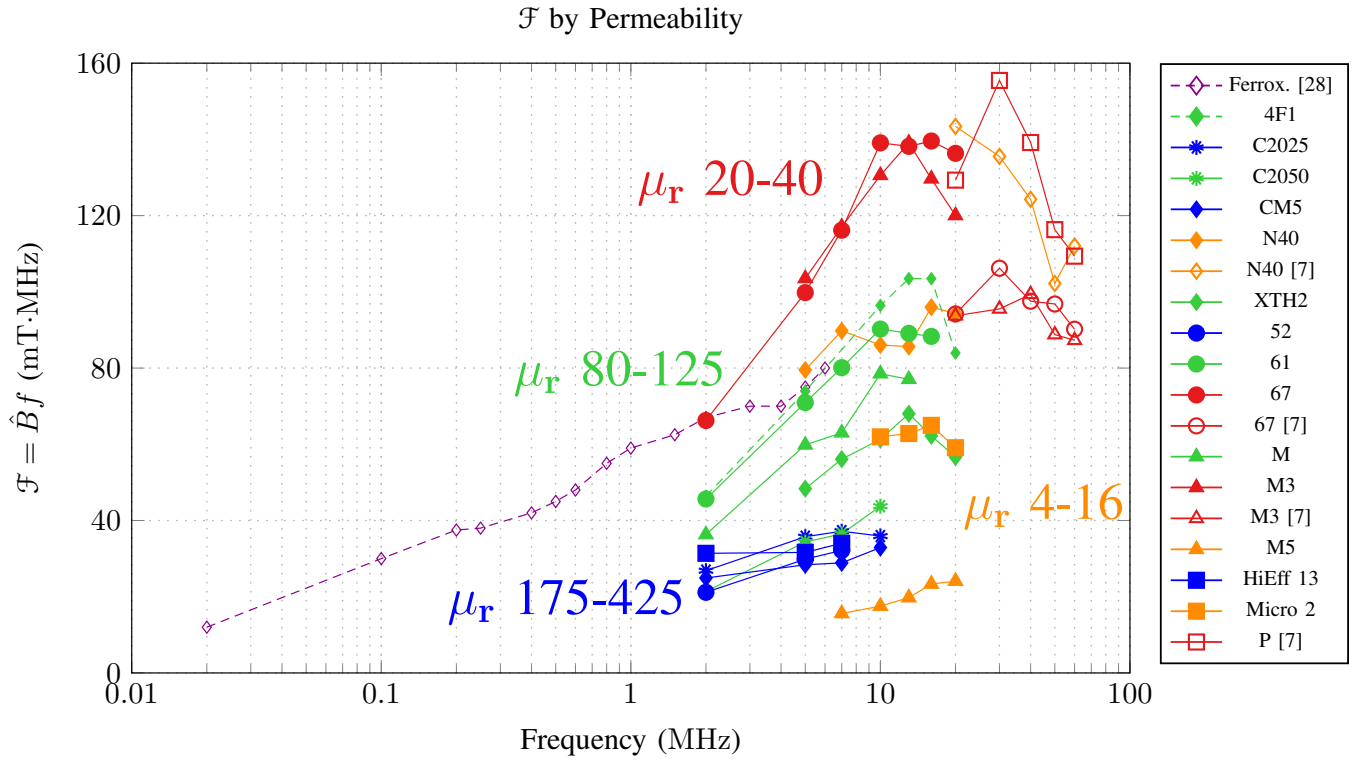


Fig. 5: Performance factor sorted by permeability. Curves shown in orange are for relative permeabilities of 4–16, those in red are for relative permeabilities of 20–40, in green for relative permeabilities of 80–125 and in blue for relative permeabilities of 175–425. It can be seen that materials having permeabilities of 20–40 often have the highest performance factor in the HF range.

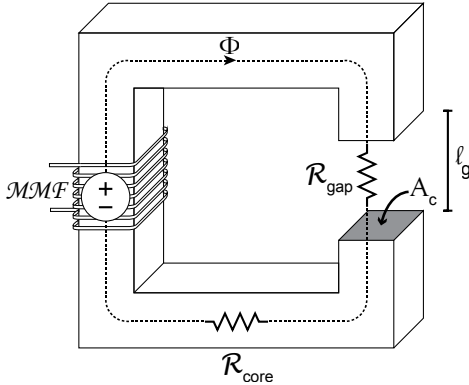


Fig. 6: Magnetic Circuit for Inductors

component designs at HF, whether there is some sacrifice made by using low permeability materials in general, and the extent to which permeability can be reduced before design becomes problematic. In this section we demonstrate that, in general, only very modest permeabilities are needed for effective magnetics design and that higher permeabilities cease to become beneficial in design.

The impact of permeability may be shown most easily for the case of an inductor with a target impedance. The inductance of an ungapped inductor is given by

$$L_{ungapped} = \frac{N^2}{\mathcal{R}_{core}} = \frac{\mu_0 \mu_r N^2 A_c}{l_c} \quad (3)$$

where \mathcal{R}_{core} is the core reluctance, N is the number of turns, A_c is the core cross-sectional area, and l_c is the flux path length through the core (Fig. 6 with $l_g = 0$). From (3) one may surmise that a higher μ_r could be directly traded for lower N to reduce copper loss at little or no expense. However, achieving minimum loss in an inductor almost always requires a *gapped inductor* to reduce core loss [30]. With a high permeability material, the reluctance in the flux path is usually dominated by the gap, and the inductance is approximated by

$$L_{gapped} \approx \frac{N^2}{\mathcal{R}_{gap}} = \frac{\mu_0 N^2 A_g}{l_g} \quad (4)$$

where \mathcal{R}_{gap} , A_g and l_g are the *gap* reluctance, cross-sectional area and length respectively. Here it is clear that permeability has little influence on design.

However, with lower permeability materials like the high-performance materials in Fig. 5, the reluctance of the gap may not be completely dominant, and the inductance is given by

$$L_{gapped} = \frac{N^2}{\mathcal{R}_{tot}} = \frac{\mu_0 N^2 A_g}{l_g + \frac{l_c}{\mu_r}} \quad (5)$$

From (5) we see that as permeability decreases, l_g must also decrease in order to maintain the same inductance (if, hypothetically, permeability could be varied independently of other material parameters). Doing so also maintains the same flux density. Thus, the performance is not affected, until the required gap length reaches zero. Further decreases in permeability cannot be accommodated by adjusting the gap length, and so the desired balance between core loss and winding loss cannot be maintained – an increase in the number of turns is needed in order to maintain the inductance, and this necessitates an increase in winding loss. Thus there is a permeability threshold above which further increases in permeability change the gap size but do not affect performance. Below that point, decreases in permeability do hurt performance because of the increase in N needed to maintain inductance. The threshold permeability is simply that which provides the specified inductance with a number of turns that provides a good tradeoff between core loss and winding loss without a gap. Based on (3), the threshold permeability is given by

$$\mu_{r,threshold} = \frac{Ll_c}{\mu_0 N^2 A_c} \quad (6)$$

Thus we see diminishing returns on increasing permeability in the design of magnetic components. In the inductor case, the advantage of additional permeability decays to zero at a finite value of permeability, $\mu_{r,threshold}$. In the case of a transformer with finite magnetizing inductance, the effect of permeability to increase the shunt path impedance will exhibit a similar effect. Although the advantage in that case will never decay to zero, it will become insignificant above a certain permeability, depending on the application.

VI. CONCLUSION

The drive to increase frequency in power conversion circuits, enabled by advanced circuit designs and wide-band-gap semiconductors, is primarily predicated on the idea that passive components can be made smaller and cheaper, and that systems can achieve higher performance. The extent to which power magnetic components can be improved at higher frequencies hinges on their loss behavior over frequency. Determining this requires information on the loss behavior of the available magnetic materials. We have undertaken measurements to produce the necessary data, and the results suggest that significant improvements in performance are possible through operation at HF using commercially available magnetic materials. Performance factor and modified performance factor facilitate understanding the implications of these data for selecting an operating frequency and understanding what is achievable. Finally, we conclude that an upper bound exists on the amount of relative permeability necessary to develop optimized cored magnetic designs, and use of high-performance materials with low permeability does not pose a disadvantage for many designs.

APPENDIX CORE LOSS MEASUREMENT METHODS

Core loss measurement approaches may be divided into calorimetric methods [31]–[37] and electrical methods, which include the classical two-winding method [30]–[33], [38], [39] and resonant techniques [7], [40]–[43]. The two-winding method is sensitive to phase errors, which become increasingly difficult to control at higher frequencies. Phase errors can be reduced by adding a resonant capacitor to the drive winding and using the sum of the sense winding voltage and the capacitor voltage for the voltage measurement [40], [42]. A variation on this approach uses an air-core transformer in place of the capacitor to cancel the reactive component over a wider frequency range [41], [42]. Although the sensitivity to phase error is reduced by the methods of [40]–[42], the phase information is still necessary in the measurement. An alternative to two-winding methods is the resonant Q measurement approach in [7]. Either approach can be accurate in the HF range, but in the resonant Q approach phase measurement is not required, eliminating that source of error.

For the above reasons, we elected to use the resonant Q approach from [7], since it is suitable for accurate measurements in the HF range. The measurement setup consists of an RF power amplifier source in series with a high- Q resonant tank, as in Fig. 7. Due to the low impedance of the measurement circuit at resonance, a $50\ \Omega$ to $3\ \Omega$ transmission line transformer (AVTECH AVX-M4) is used to better match the output impedance of the power amplifier. A low- Q parallel resonant filter is also added to remove any harmonic components from the input to the measurement circuit. These components are simply added to ensure that the input voltage to the measurement circuit is a single-frequency sinusoid. As will be described, the measurement itself only depends on $v_{in,pk}$ and $v_{out,pk}$, so the actual implementation to the left of the dotted line in Fig. 7 is immaterial so long as good drive waveform quality is obtained.

The voltage at the input to the tank and the output voltage (i.e. the voltage across the resonant capacitor) are measured with respect to ground. At the undamped resonant frequency $\omega_r = 1/\sqrt{LC}$ the quality factor of the inductor is simply the ratio of the output to the input voltage amplitudes

$$\begin{aligned} \frac{V_{out-pk}}{V_{in-pk}} &= \left| \frac{R_C + \frac{1}{j\omega_r C_m}}{R_{core} + R_{cu} + R_C} \right| \approx \frac{\omega_r L_m}{R_{core} + R_{cu}} \\ &= Q_{L_m} \end{aligned} \quad (7)$$

where R_C is the equivalent series resistance (ESR) of the capacitor, and R_{cu} and R_{core} are equivalent series resistances representing winding (copper) loss and core loss, respectively. In the above derivation, the reactance of the capacitor cancels that of the inductor at the resonant frequency. The approximation is also made that the capacitor equivalent series resistance is small with respect to the modeled inductor resistance.

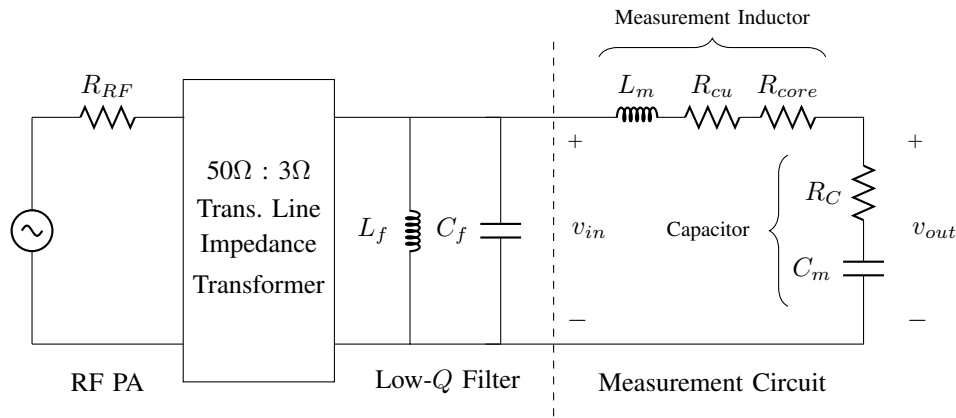


Fig. 7: Circuit schematic used for core loss measurement.

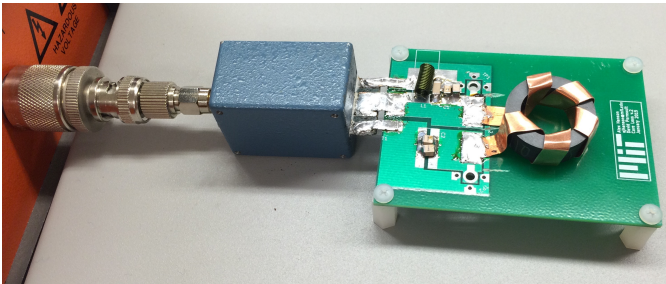


Fig. 8: Image of a test circuit in operation. The power amplifier (orange, left) connects to the board through the transmission line transformer (blue). The input filter, measurement inductor, and resonant capacitor are visible.

The circuit resistance modeling core loss can be calculated from measured values

$$R_{core} = \frac{2\pi f_s L V_{in-pk}}{V_{out-pk}} - R_C - R_{cu} \quad (8)$$

where the copper resistance is estimated from measurements of an air-core inductor of identical construction and/or through numerical modeling. The current through the inductor and capacitor is the same (and known from the measured $V_C = V_{out}$) so volumetric power loss can be computed directly:

$$P_V = \frac{I_{L-pk}^2 R_{core}}{2V_L} \quad (9)$$

Possible sources of error and mitigation strategies are covered in [7]. This approach can yield core loss measurements that are accurate to better than 20%, which is sufficient for design purposes and within the lot-to-lot variation of typical materials.

ACKNOWLEDGMENT

This work was made possible by funding from Lockheed Martin under the Massachusetts Institute of Technology Energy Initiative and by a gift from Texas Instruments.

REFERENCES

- [1] D. Harburg, X. Yu, F. Herrault, C. Levey, M. Allen, and C. Sullivan, "Micro-fabricated thin-film inductors for on-chip power conversion," in *7th International Conference on Integrated Power Electronics Systems (CIPS)*. IEEE, 2013, pp. 6–8.
- [2] D. Perreault, J. Hu, J. Rivas, Y. Han, O. Leitermann, R. Pilawa-Podgurski, A. Sagneri, and C. Sullivan, "Opportunities and challenges in very high frequency power conversion," in *Twenty-Fourth Annual IEEE Applied Power Electronics Conference and Exposition (APEC)*, Feb 2009, pp. 1–14.
- [3] M. Araghchini, J. Chen, V. Doan-Nguyen, D. Harburg, D. Jin, J. Kim, M. Kim, S. Lim, B. Lu, D. Piedra, J. Qiu, J. Ranson, M. Sun, X. Yu, H. Yun, M. Allen, J. del Alamo, G. DesGroseilliers, F. Herrault, J. Lang, C. Levey, C. Murray, D. Otten, T. Palacios, D. Perreault, and C. Sullivan, "A technology overview of the powerchip development program," *IEEE Transactions on Power Electronics*, vol. 28, no. 9, pp. 4182–4201, 2013.
- [4] C. Mathuna, N. Wang, S. Kulkarni, R. Anthony, C. N. J. Oliver, P. Alou, V. Svikovic, J. Cobos, J. Cortes, F. Neveu, C. Martin, B. Allard, F. Voiron, B. Knott, C. Sandner, G. Maderbacher, J. Pichler, M. Agostinelli, A. Anca, and M. Breig, "Power supply with integrated passives - the eu fp7 powerswipe project," in *8th International Conference on Integrated Power Electronics Systems (CIPS)*. IEEE, 2014, pp. 25–27.
- [5] R. Pilawa-Podgurski, A. Sagneri, J. Rivas, D. Anderson, and D. Perreault, "Very high frequency resonant boost converters," in *Power Electronics Specialists Conference, 2007. PESC 2007. IEEE*, June 2007, pp. 2718–2724.
- [6] J. Hu, A. Sagneri, J. Rivas, Y. Han, S. Davis, and D. Perreault, "High frequency resonant sepic converter with wide input and output voltage ranges," in *Power Electronics Specialists Conference, 2008. PESC 2008. IEEE*, June 2008, pp. 1397–1406.
- [7] Y. Han, G. Cheung, A. Li, C. Sullivan, and D. Perreault, "Evaluation of magnetic materials for very high frequency applications," *IEEE Transactions on Power Electronics*, pp. 425–435, 2008.
- [8] S. A. Mulder, "Fit formulae for power loss in ferrites and their use in transformer design," in *Proceedings of the International Power Conversion Conference*, 1993, pp. 345–345.
- [9] S. A. Mulder, "Loss formulas for power ferrites and their use in transformer design," *Philips Components*, p. 16, 1994, also in *PCIM 1995*.
- [10] T. G. W. Stijntjes, "Power ferrites: Performance and microstructure," in *ICF5*, no. C1-01, 1989, p. 587.
- [11] L. Bosley, "Data sheets provide clues for optimizing selection of smps ferrite core material," in *PCIM*, vol. 19, 1993, pp. 13–13.
- [12] A. Goldman, *Modern ferrite technology*. Springer, 2006.
- [13] F. Alves, R. Lebourgeois, and T. Waeckerle, "Soft magnetic materials for electrical engineering: State of the art and recent advances," *European transactions on electrical power*, vol. 15, no. 6, pp. 467–479, 2005.

- [14] "Soft ferrite cores: A user's guide," 2011. [Online]. Available: <http://www.transformer-assn.org/Soft\Ferrite\Cores\User\%20Guide.pdf>
- [15] F. Forest, E. Laboure, T. Meynard, and M. Arab, "Analytic design method based on homothetic shape of magnetic cores for high-frequency transformers," *Power Electronics, IEEE Transactions on*, vol. 22, no. 5, pp. 2070–2080, 2007.
- [16] T. M. Undeland, J. Lode, R. Nilssen, W. P. Robbins, and N. Mohan, "A single-pass design method for high-frequency inductors," *Industry Applications Magazine, IEEE*, vol. 2, no. 5, pp. 44–51, 1996.
- [17] M. Bogs and W. Holubarsch, "Design principles for high frequency power transformer materials," *Le Journal de Physique IV*, vol. 7, no. C1, pp. C1–117, 1997.
- [18] M. S. Rylko, B. J. Lyons, J. G. Hayes, and M. G. Egan, "Revised magnetics performance factors and experimental comparison of high-flux materials for high-current dc-dc inductors," *Power Electronics, IEEE Transactions on*, vol. 26, no. 8, pp. 2112–2126, 2011.
- [19] D. Yao and C. Sullivan, "Effect of capacitance on eddy-current loss in multi-layer magnetic films for mhz magnetic components," in *IEEE Energy Conversion Congress and Exposition (ECCE)*. IEEE, 2009, pp. 1025–1031.
- [20] M. E. Dale and C. R. Sullivan, "Comparison of power loss in single-layer and multi-layer windings with physical constraints or strong harmonics," in *IEEE International Symposium on Industrial Electronics*, 2006, pp. 1467–1473.
- [21] W. Hurley, E. Gath, and J. Breslin, "Optimizing the ac resistance of multilayer transformer windings with arbitrary current waveforms," *IEEE Transactions on Power Electronics*, vol. 15, no. 2, pp. 369–376, Mar 2000.
- [22] C. R. Sullivan, "Layered foil as an alternative to litz wire: Multiple methods for equal current sharing among layers," in *IEEE 15th Workshop on Control and Modeling for Power Electronics (COMPEL)*, June 2014, pp. 1–7.
- [23] S. Lim, D. Otten, and D. Perreault, "Power conversion architecture for grid interface at high switching frequency," in *Applied Power Electronics Conference and Exposition (APEC), 2014 Twenty-Ninth Annual IEEE*, March 2014, pp. 1838–1845.
- [24] S. Lim, D. Otten, and D. Perreault, "Ac-dc power factor correction architecture suitable for high frequency operation," *IEEE Transactions on Power Electronics*, IEEE Early Access.
- [25] E. C. Snelling, *Soft Ferrites, Properties and Applications*, 2nd ed. Butterworths, 1988.
- [26] C. Sullivan, "Optimal choice for number of strands in a litz-wire transformer winding," *Power Electronics, IEEE Transactions on*, vol. 14, no. 2, pp. 283–291, Mar 1999.
- [27] C. R. Sullivan and R. Y. Zhang, "Simplified design method for litz wire," in *IEEE Applied Power Electronics Conference and Exposition (APEC)*. IEEE, 2014, pp. 2667–2674.
- [28] "Soft ferrites and accessories data handbook," Ferroxcube International Holding B.V., Tech. Rep., 2013.
- [29] C. P. Steinmetz, "On the law of hysteresis," *American Institute of Electrical Engineers, Transactions of the*, vol. IX, no. 1, pp. 1–64, Jan 1892.
- [30] A. van den Bossche and V. Valchev, *Inductors and Transformers for Power Electronics*. Taylor and Francis Group, 2005.
- [31] IEEE, "Ieee standard for test procedures for magnetic cores, standard 393-1991," Tech. Rep., 1992.
- [32] IEC, "Cores made of soft magnetic materials-measuring methods, international standard 62044-1," Tech. Rep., 2002-2005.
- [33] A. Goldberg, "Development of magnetic components for 1-10 mhz dc/dc converters," Ph.D. dissertation, Massachusetts Institute of Technology, 1988.
- [34] C. Xiao, G. Chen, and W. G. Odendaal, "Overview of power loss measurement techniques in power electronics systems," *IEEE Transactions on Industry Applications*, vol. 43, no. 3, pp. 657–664, 2007.
- [35] D. Christen, U. Badstuebner, J. Biela, and J. Kolar, "Calorimetric power loss measurement for highly efficient converters," in *2010 International Power Electronics Conference (IPEC)*. IEEE, 2010, pp. 1438–1445.
- [36] J. Miller, C. Ayers, L. Seiber, and D. Smith, "Calorimeter evaluation of inverter grade metalized film capacitor esr," in *IEEE Energy Conversion Congress and Exposition (ECCE)*, Sept 2012, pp. 2157–2163.
- [37] R. Linkous, A. Kelley, and K. Armstrong, "An improved calorimeter for measuring the core loss of magnetic materials," in *Applied Power Electronics Conference and Exposition, 2000. APEC 2000. Fifteenth Annual IEEE*, vol. 2. IEEE, 2000, pp. 633–639.
- [38] V. J. Thottuvelil, T. G. Wilson, and H. Owen Jr, "High-frequency measurement techniques for magnetic cores," *IEEE Transactions on Power Electronics*, vol. 5, no. 1, pp. 41–53, 1990.
- [39] T. Sato and Y. Sakaki, "100 kHz-10 MHz iron loss measuring system," *IEEE Transactions on Magnetics*, vol. 23, no. 5, pp. 2593–2595, 1987.
- [40] M. Mu, Q. Li, D. Gilham, F. C. Lee, and K. D. Ngo, "New core loss measurement method for high frequency magnetic materials," in *IEEE Energy Conversion Congress and Exposition (ECCE)*. IEEE, 2010, pp. 4384–4389.
- [41] M. Mu, F. C. Lee, Q. Li, D. Gilham, and K. D. Ngo, "A high frequency core loss measurement method for arbitrary excitations," in *IEEE Applied Power Electronics Conference and Exposition (APEC)*. IEEE, 2011, pp. 157–162.
- [42] D. Hou, M. Mu, F. Lee, Q. Li *et al.*, "New core loss measurement method with partial cancellation concept," in *IEEE Applied Power Electronics Conference and Exposition (APEC)*. IEEE, 2014, pp. 746–751.
- [43] C. Foo and D. Zhang, "A resonant method to construct core loss of magnetic materials using impedance analyser," in *IEEE Power Electronics Specialists Conference (PESC)*, vol. 2. IEEE, 1998, pp. 1997–2002.